Front. Environ. Sci. Eng. 2022, 16(12): 157
https://doi.org/10.1007/s11783-022-1592-x

RESEARCH ARTICLE

Effect of wetland plant fermentation broth on nitrogen removal and bioenergy generation in constructed wetland-microbial fuel cells

Yiting Chen[1,2], Jun Yan[1,2], Mengli Chen[1,2], Fucheng Guo[1,2], Tao Liu[1,2], Yi Chen (✉)[1,2]

1 Key Laboratory of the Three Gorges Reservoir Region's Eco-Environment (Ministry of Education), Chongqing University, Chongqing 400045, China
2 College of Environment and Ecology, Chongqing University, Chongqing 400045, China

HIGHLIGHTS

- Fermentation broth facilitates N removal and energy yields in tertiary CW-MFC.
- Carbon sources are preferred for nitrogen removal over electricity generation.
- A mutual promotion relationship exists between acetic and humic acid in N removal.
- Humic acid boosts the abundances of functional genes relate to nitrogen metabolism.

GRAPHIC ABSTRACT

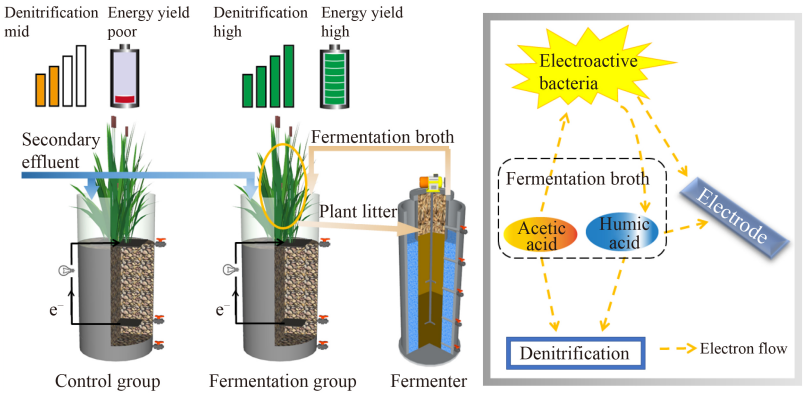

ARTICLE INFO

Article history:
Received 29 January 2022
Revised 27 April 2022
Accepted 16 May 2022
Available online 25 June 2022

Keywords:
Constructed wetland
Microbial fuel cell
Nitrogen removal
Bioenergy generation
Carbon source

ABSTRACT

Constructed wetlands (CWs) are widely used as a tertiary treatment technology, and the addition of carbon sources can significantly improve advanced nitrogen removal. However, excessive carbon sources would lead to an increase in the effluent chemical oxygen demand in CWs, and microbial fuel cells (MFCs) can convert these into electricity. In this study, constructed wetland-microbial fuel cells (CW-MFCs) were built to achieve simultaneous nitrogen removal and electricity generation, using wetland plant litter fermentation broths as carbon sources. The total nitrogen removal in the groups with fermentation broth addition (FGs) reached 83.33%, which was 19.64% higher than that in the CG (group without fermentation broth), and the mean voltages in the FGs were at least 2.6 times higher than that of the CG. Furthermore, two main components of the fermentation broths, acetic acid (Ac) and humic acid (HA), were identified using a three-dimensional excitation emission matrix and gas chromatograph and added to CW-MFCs to explore the influence mechanism on the treatment performance. Denitrification and electrogenesis presented the same tendency: Ac&HA > Ac > CG' (groups without Ac and HA). These results indicate that Ac and HA increased the abundance of functional genes associated with nitrogen metabolism and electron transfer. This study demonstrated that CW-MFC fermentation broth addition can be a potential strategy for the disposal of secondary effluent and bioelectricity generation.

1 Introduction

Eutrophication occurs easily when the water contains excessive nitrogen and phosphorus (Chen et al., 2014b; Chen et al., 2020). Water eutrophication caused by nitrogen has been reported to occur frequently in some rivers (Hansen et al., 2018). Nitrogen in the secondary effluent of wastewater treatment plants (WWTPs) is an influential source of pollution for receiving water bodies

✉ Corresponding author
E-mail: chenyi8574@cqu.edu.cn

(Zhou et al., 2021). Therefore, the advanced treatment of nitrogen in secondary effluents is critical.

Constructed wetland (CW-MFC) is widely used for wastewater treatment, since it inherits the treatment of pollutants from constructed wetland (CW), and yields electricity as a microelectrochemical technology. The process of producing electricity might be beneficial for denitrification because the electrons produce in anodic area are transferred to the cathode, then the bacteria on the cathode can use those electrons for denitrification (Puig et al., 2012). For instance, Ma et al. (2015) indicated that the captured electrons would drive the denitrification process at the cathode area, and Dash and Chaudhari (2005) found that the nitrate transformation rate is positively related to current density. Researchers have conducted related studies on CW-MFCs treating low C/N ratio wastewater. Zhao et al. (2020) utilized CW-MFCs to treat secondary effluent containing Pb (II) and found that Pb (II) promotes power generation while inhibiting ammonia removal. Wang et al. (2019) treated low C/N ratio wastewater and discovered that the total nitrogen (TN) effluent concentration was close to 10 mg/L, and the output voltage was approximately 60 mV. However, 10 mg/L TN was still a threat to water eutrophication in backwaters dominated by tailwater. Related results showed that CW-MFCs could not completely relieve the limitation of insufficient carbon sources for denitrification, so addition of carbon sources is necessary.

Soluble carbon sources, such as ethanol, glucose, cellulose, and acetate, were the most frequent additive (Zhu et al., 2014). However, soluble carbon sources are expensive and may cause secondary pollution (Yuan et al., 2020). Solid carbon sources, such as wheat straw, corn stalks, cotton, poly (butylene succinate), newspaper, and rice husks, have also been utilized for treating low C/N ratio wastewater (Wang et al., 2009; Chen et al., 2014a; Si et al., 2018; Tao et al., 2021). However, these solid carbon sources would lead to inconsistent carbon release in different stages (Zhang et al., 2016), and consequently, only a small portion of the solid carbon sources actually participated in the nitrogen transformation (Chen et al., 2014a). Moreover, inappropriate supplementation of solid carbon would result in the clogging of reactors, which is a fatal issue for these systems (Zhao et al., 2017). Thus, identifying effective carbon sources is urgently necessary. According to the literature, the rate of plant litter accumulation in mature wetlands has reached 500–2000 g C/(m^2·yr) (Hume et al., 2002). However, these abundant carbon sources could not be released into the CWs because of the barrier of the surface gravel layers. For promoting the recycling of waste resources, wetland plant litter was converted into fermentation broths (Fu et al., 2018). Volatile fatty acids (VFAs), such as acetic acid (Ac), are important components of fermentation broths and can supplement denitrifying carbon sources (Zhang et al., 2016). Humic acid (HA) and other macromolecules are also components of the fermentation broth (Luo et al., 2021), and the effects on denitrification and electricity generation in CW-MFCs remain unknown.

As is well-known, the performances of nitrogen removal in CW and power generation in microbial fuel cell (MFC) will be enhanced after adding carbon sources. However, the effects of fermentation broths on denitrification and electricity generation in CW-MFCs remain unknown, especially for the relationships between denitrification and power generation. Whether the exoelectrogens and denitrifiers will compete for carbon sources in CW-MFC, relevant research is a state of absence. Therefore, it is necessary to carry out the effect mechanism of fermentation broth on CW-MFC.

Herein, wetland plant litter (*Typha latifolia*) fermentation broths at four different periods were prepared and added to CW-MFC systems to investigate their influence on nitrogen removal and bioenergy generation. Furthermore, the influence mechanism was explored by adding the two main components of the fermentation broths to the CW-MFC systems. We aimed to explore (i) the temporal variation in the main components of the fermentation broths, (ii) whether the addition of fermentation broths can facilitate the denitrification and power generation capacity of CW-MFCs, and (iii) the determinants in fermentation broths that promote the advanced nitrogen removal and power generation of CW-MFCs.

2 Materials and methods

2.1 Preparation of fermentation broth

To prepare the fermentation broths, we used litter from a common wetland plant, *Typha latifolia*, as the plant carbon source. The mass ratio of the stems and leaves of *Typha latifolia* was 1:1. The stems and leaves were dried, cut to 1–2 cm, sealed, and stored for later use.

The fermentation tank (volume, 20 L) is shown in Fig. 1. The fermentation mixtures comprised 400 g (dry weight) of wetland plant litter, 2 L of inoculated sludge, and 18 L of tap water; next, all of them were placed into a fermentation tank for fermenting. In addition, trace metals (e.g., Ni^{2+}, Co^{2+}) and mineral salts (e.g., Ca^{2+}, K^{+}) were added to the fermentation tank (Fu et al., 2017). Inoculated sludge was collected from the anaerobic zone of the A/A/O oxidation ditch of the Jingkou Municipal WWTP, Chongqing, China.

After fermentation, the fermentation tank was sealed with rubber rings and the fermentation temperature was maintained at 30 ± 3 °C. To ensure homogeneous mixing, we inserted a stainless steel blender connected to an electric motor into the fermentation tank at a stirring speed of 150 r/min. From the 5th day, an aliquot of 2.5 L fermentation broth was removed from the fermentation tank every 5 d for 20 d (5 d, 10 d, 15 d, and 20 d).

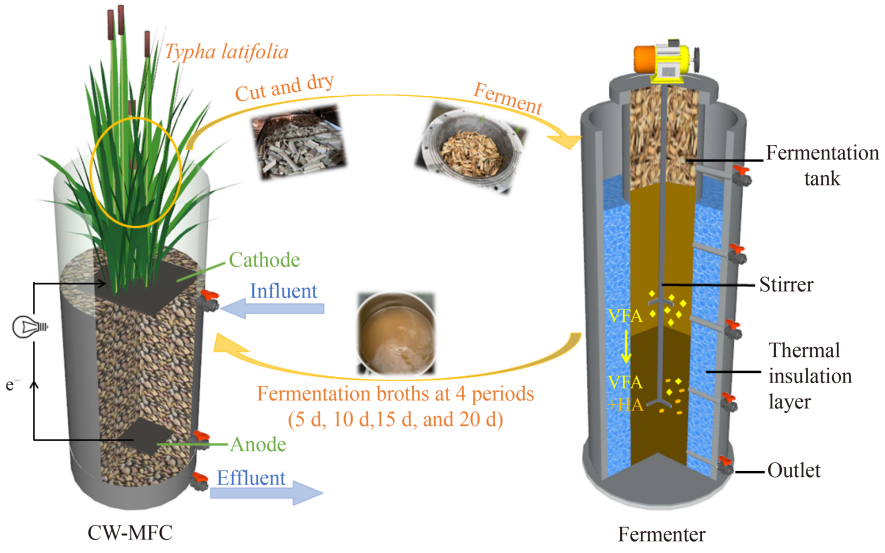

Fig. 1 Schematic diagram of experimental setup.

Fermentation broths were sealed and stored in a refrigerator at −20 °C for later use.

2.2 CW-MFCs construction, inoculation and operation

As shown in Fig. 1, the reactors were constructed using cylindrical containers (polymethyl methacrylate, inner diameter 20 cm, height 50 cm). Lab-scale CW-MFCs filled with gravel (particle size: 6–8 mm) were established. The water outlet and sampling ports were at the bottom of the reactors, and the water inlet was set 20 cm from the top of the reactors. The influent flowed downward from the top of the reactors. Both the anode and cathode materials were carbon fiber felts that adhered to stainless steel wire meshes, and the thickness of the carbon fiber felts was 10 mm. The spacing between the anode and cathode was 20 cm, and they were connected to an external resistor (1000 Ω). The anode was placed 10 cm above the bottom of the CW-MFC reactor. *Typha latifolia* was planted in each CW-MFC at a density of two plants per reactor.

The CW-MFCs were inoculated with anaerobic active sludge (2 L) obtained from the Jingkou Municipal WWTP, Chongqing, China. Effluent flow velocity should be well controlled during the inoculation period to avoid sludge loss. Synthetic secondary effluents were added to the reactors three months in advance to ensure that the CW-MFC systems were stable. This experiment was operated in batch mode, and the hydraulic retention time was three days. Two parallel groups were set both in Period I and II, and each experimental condition runed for five cycles. The reactors were initiated in August 2020.

2.3 Preparation of synthetic wastewater

The main components of the synthetic secondary wastewater were COD (60 mg/L), NO_3^--N (12 mg/L), and NH_4^+-N (8 mg/L). In addition, trace metals (e.g., Ni^{2+}, Co^{2+}) and mineral salts (e.g., Ca^{2+}, K^+) are required. An effective volume of 5 L synthetic wastewater was required for each reactor.

The experiment was conducted in two parts. Period I explored whether the addition of fermentation broth can facilitate the denitrification and power generation capacity of CW-MFC, which included five experimental conditions (no fermentation broth (CG), and 0.5 L of 5 d (FG-5), 10-d (FG-10), 15 d (FG-15), and 20 d (FG-20) fermentation broths added to 9.5 L synthetic wastewater). Period II focused on the mechanism of the influence of the two main components (Ac and HA) of fermentation broths on the denitrification and power generation capacity of CW-MFCs. The experimental conditions included pure synthetic wastewater (CG') and synthetic wastewater injected with 30 mg/L Ac (Ac), 30 mg/L Ac, and 2.5 mg/L HA (Ac&HA). HA was purchased from Aladdin Chemistry Co. Ltd. (Shanghai, China).

2.4 Analytical methodology

2.4.1 Fermentation broth composition analysis

To analyze the composition of fermentation broths, we collected water samples from the fermenter at 5 d, 10 d, 15 d, and 20 d and then filtered them through 0.45 μm filter membranes. A portion of each filtrate was used to measure total organic carbon (TOC). Each of the remaining filtrates was diluted accordingly to standardize their TOC to 10 mg/L for three-dimensional excitation emission matrix (3D-EEM, Hitachi F-7000) fluorescence spectroscopy (Luo et al., 2021). The instrument parameter settings were as follows: excitation wavelength (Ex) was changed from 220 nm to 400 nm, emission wavelength (Em) was changed from 230 nm to 550 nm, and both Ex

and Em sampling intervals were 5 nm.

VFAs in the fermentation broths were tested using a gas chromatograph (GC1690, SHIMADZU) equipped with a flame ionization detector and a DB-FFAP capillary column. The temperatures of the sample injector and detector were maintained at 140 °C. The initial temperature was 100 °C, which was maintained for 3 min, and then increased to 172 °C at a rate of 6 °C/min and maintained for 2 min. Standard samples were prepared using chromatographically pure formic acid, acetic acid, propionic acid, isobutyric acid, butyric acid, isovaleric acid, and valeric acid. The VFA concentration was calculated using an N2000 chromatographic workstation with an external standard method.

2.4.2 Water quality determination and microbiological analysis

Influent and effluent samples were collected before the beginning of each batch. The COD, NH_4^+-N, NO_3^--N, and TN concentrations were measured using standard methods (APHA, 1998). The dissolved oxygen (DO) and pH were periodically measured using a DO/pH probe connected to a DO meter (WTW Oxi 3310 IDS, Germany) and pH meter (WTW pH 3310 IDS, Germany), respectively.

At the end of this experiment, gravel samples were collected from the CW-MFC reactors. The gravel samples were then separated by shaking at 225 r/min for 3 h in phosphate buffered solution (Yan et al., 2021; Guo et al., 2022). The microbial samples were stored in a refrigerator at −80 °C. The 515FmodF (5'-GTGYCAGCMGGCGC-GCGGTAA-3') and 806RmodR (5'-GGACTACNGGGT-WTAT-3') were used to amplify the V4 high-variation zone (291 bp) of the 16S rRNA gene. Functional gene abundances related to nitrogen metabolism and electron transfer were predicted using PICRUSt2, which was based on 16S rRNA. Please refer to the Supplementary Material for details.

2.4.3 Electrochemical calculations

The data collection system (PS2016) was utilized to record the voltage every 10 min. When measuring the polarization curve, the external resistance was increased from 25 to 9999 Ω (Oon et al., 2018). Current density (J) and power density (P) were calculated as

$$J = U/(R_{ext} \cdot A), \quad (1)$$

$$P = J \cdot U, \quad (2)$$

where U is the voltage (V), R_{ext} is the external resistance (1000 Ω), and A is the electrode size (0.015 m^2 in this study). In addition, the internal resistances of the CW-MFC reactors were determined by the polarization curve because the internal resistances could be calculated at the maximum power density.

The coulombic efficiency (CE) was calculated by Eq. (3) (Oon et al., 2018).

$$CE = (M \times I)/(F \times V \times b \times \Delta COD), \quad (3)$$

where M is the molecular weight of oxygen (M = 32), I represents the current (A), F is Faraday's constant (F = 94685), V represents the liquid volume in the CW-MFC (V = 4 L in this study), b represents the number of electrons donated by one mole of O_2 (b = 4), and ΔCOD represents the decrease in COD (mg/L).

2.5 Statistical analysis

Statistical analysis was performed using SPSS (version 20.0). All the analyses were repeated to ensure data precision. The results are presented as mean ± standard deviation (s.d.). The difference between the two groups was determined using one-way variance analysis. A significant difference was indicated when $p < 0.05$.

3 Results

3.1 Fermentation broth composition analysis

The 3D-EEM of the fermentation broths at different periods (5 d, 10 d, 15 d, and 20 d) is shown in Fig. 2. In general, the response regions of organic matter to emission and excitation waves in soluble organic matter can be divided into four main categories: aromatic proteins (I, II), fulvic acid-like (III), soluble microbial by-product-like (IV), and humic acid-like (V). The graphs were plotted after the fluorescence intensities were unified so that the relative concentrations could be qualitatively determined based on the peak sizes. Each fermentation broth had two peaks located in region IV and region V, which represented soluble microbial by-product-like and humic acid-like, respectively. The peaks in region IV ascended first from FG-5 to FG-15 and then descended at FG-20. With an increase in the fermentation period, the peak values in region V increased, indicating that humic acid-like substances gradually accumulated.

Studies have shown that more than 85% of the soluble microbial by-product-like substances (region IV) in anaerobic fermentation were VFA (Zhang et al., 2016); thus, the VFA components in the fermentation broths were analyzed next. The VFAs contained Ac, propionic acid, butyric acid, isobutyric acid, valeric acid, and isovaleric acid (Duan et al., 2018). The VFA concentrations of the fermentation broths at different periods are presented in the supplementary materials (Fig. S1). The VFA concentrations first increased from FG-5 to FG-15 and then decreased at FG-20, which was the same result as that of 3D-EEM. The Ac concentration was much higher than that of other substances, and the concentrations of the 5 d, 10 d, 15 d, and 20 d fermentation broths were 256.38, 282.70, 369.93, and

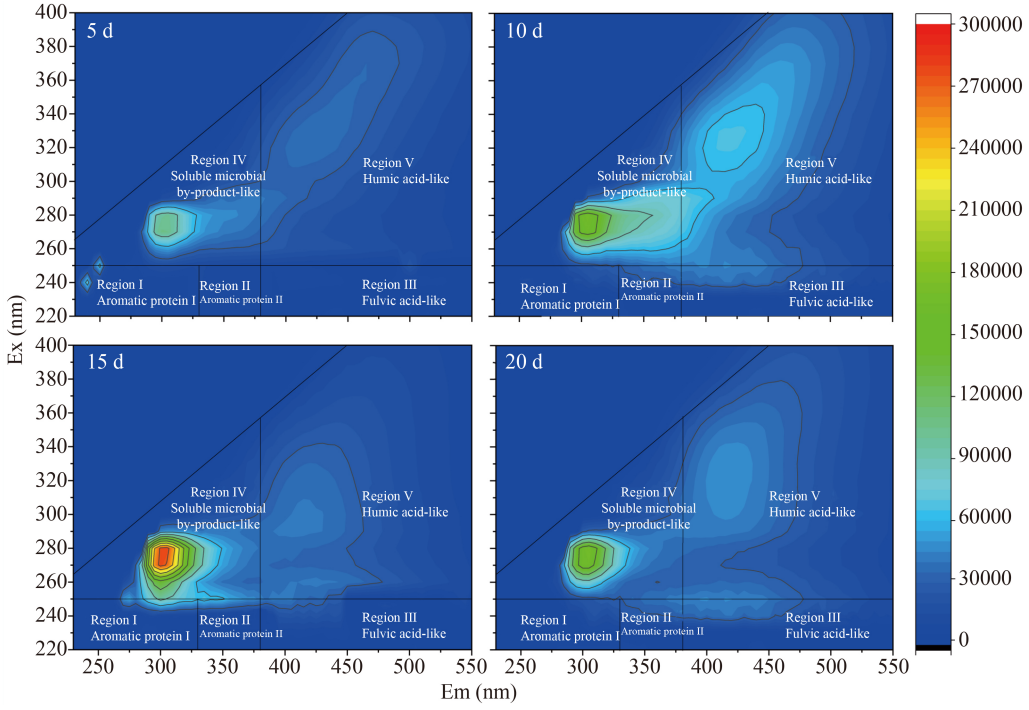

Fig. 2 3D-EEM (The fermentation periods were 5 d, 10 d, 15 d, and 20 d).

346.72 mg/L, respectively. The concentration of VFA in the 15 d fermentation broth was the highest.

3.2 Pollutant removal in CW-MFC with fermentation broth

The concentrations and pollutant removal efficiencies, including COD, NH_4^+-N, NO_3^--N, and TN, in Period I are illustrated in Fig. 3. The COD concentration of CG in influent was approximately 59.94 ± 2.95 mg/L, and that of the other 4 groups which added with fermentation broths were 93.50 ± 3.00 mg/L in Period I. The average COD concentrations in the effluents collected from CG, FG-5, FG-10, FG-15, and FG-20 were 14.72, 7.55, 5.83, 6.00, and 3.03 mg/L, respectively (showed in Fig. 3a). Only 75.44% of COD was removed in CG, and the removal efficiencies of the fermentation groups all reached more than 90% (FG-20 reached 96.68%). As demonstrated in Fig. 3b, the group with the highest removal efficiency of ammonia nitrogen was FG-15 (removal efficiency of 60.87%), which was 18.47% higher than that of CG (removal efficiency of 42.40%). The removal rate of NO_3^--N in the CG, FG-5, FG-10, FG-15, and FG-20 groups was 75.73%, 98.91%, 98.84%, 98.52%, and 98.57%, respectively (Fig. 3c). Moreover, the effluent nitrate concentration decreased from 3.24 to 0.19 mg/L. A significant difference in nitrate removal was observed among the CW-MFC reactors with or without fermentation broths ($p < 0.001$). Furthermore, Fig. 3d shows that the TN removal efficiencies of CG, FG-5, FG-10, FG-15, and FG-20 were 63.69%, 76.76%, 78.06%, 83.33%, and 81.00%, respectively. The corresponding TN concentrations in the effluents were 7.59, 5.02, 4.43, 3.47, and 3.90 mg/L. The TN removal efficiency of FG-15 was 19.64% higher than that of CG.

Because Ac and HA are the two main components of fermentation broths (showed in Fig. 2 and Fig. S1), Ac and HA were added to CW-MFCs (Period II) to further study their impacts on nitrogen removal and electricity generation. The influent COD concentration of CG' was approximately 60.88 ± 0.16 mg/L, and the other groups added with Ac and HA were 90.00 ± 3.50 mg/L in Period II, which was basically consistent with the experiment in Period I. The COD concentration of the CW-MFC effluents collected from the CG', Ac, and Ac&HA were 13.48, 3.55, and 8.74 mg/L, respectively; and the removal rates of COD in CG', Ac, and Ac&HA were 77.85%, 95.93%, and 90.31%, respectively (shown in Fig. 4a). The ammonia nitrogen removal efficiencies in the CG', Ac, and Ac&HA groups were 51.25%, 50.35%, and 55.75%, respectively, and the effluent concentrations of ammonia nitrogen in CG', Ac, and Ac&HA were 3.60, 3.56, and 3.20 mg/L, respectively (Fig. 4b). Furthermore, Fig. 4c shows that the removal rate of nitrate in CG' was only 76.30%; whilst the removal rate of Ac and Ac&HA were 97.46% and 98.31%, respectively; and the nitrate effluent concentrations of CG', Ac, and Ac&HA were 3.24, 0.35, and 0.22 mg/L, respectively. As shown in Fig. 4d, the TN removal efficiencies of CG', Ac, and Ac&HA were 67.46%, 80.07%, and 85.49%, respectively. The lowest TN effluent concentration was 3.05 mg/L which existed in Ac&HA.

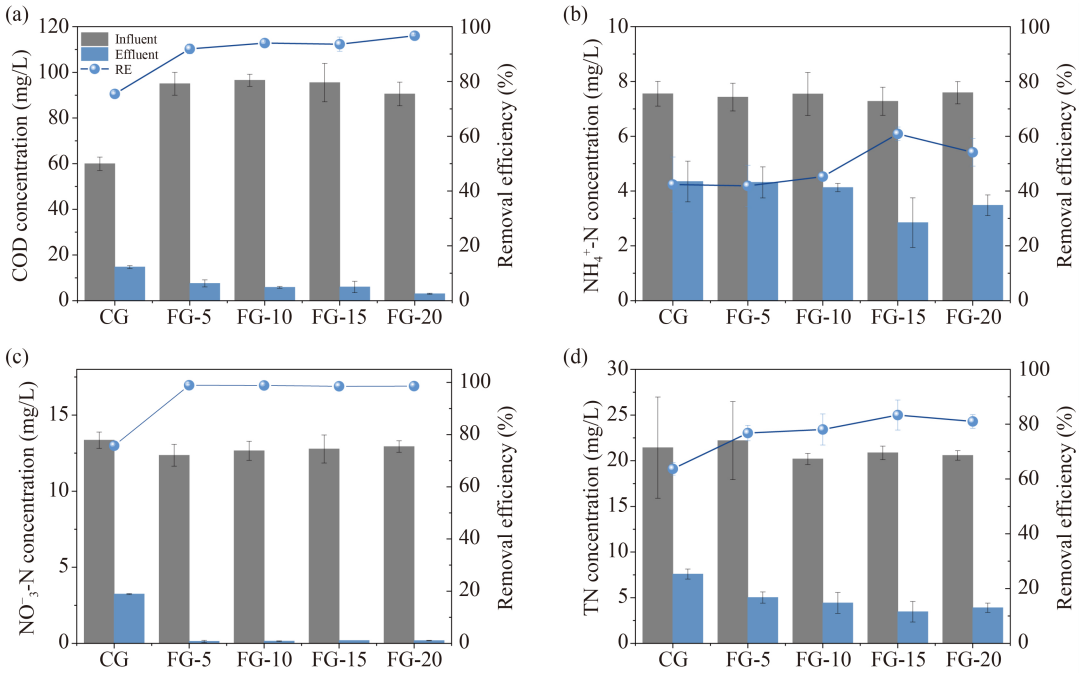

Fig. 3 The influent, effluent concentration and removal efficiency of COD, NH_4^+-N, and TN in Period I. (CG: control group without fermentation broth, FG-5: fermentation group added with 5 d fermentation broth, FG-10: fermentation group added with 10 d fermentation broth, FG-15: fermentation group added with 15 d fermentation broth, FG-20: fermentation group added with 20-d fermentation broth).

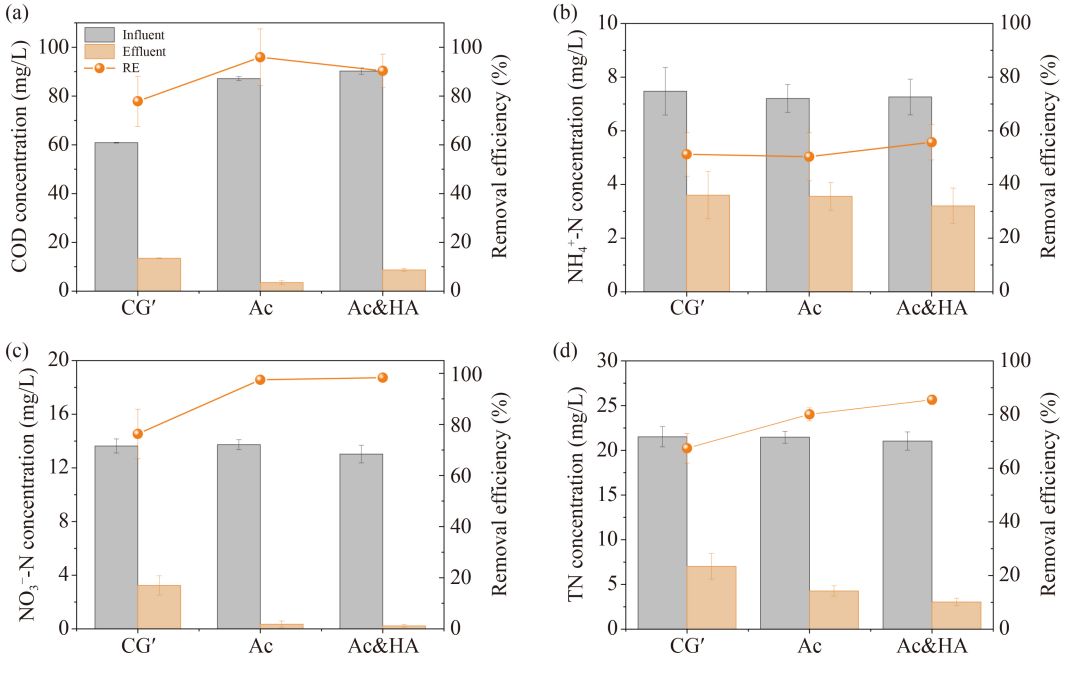

Fig. 4 The influent, effluent concentration and removal efficiency of COD, NH_4^+-N, NO_3^--N, and TN in Period II. (CG': control group without Ac and HA, Ac: added with 30 mg/L Ac, Ac&HA: added with 30 mg/L Ac and 2.5 mg/L HA).

3.3 Power generation in CW-MFC with fermentation broth

The mean voltages for Period I are shown in Fig. 5a. The mean voltages of CG, FG-5, FG-10, FG-15, and FG-20 were 43.43, 210.85, 178.55, 128.51, and 119.18 mV, respectively. The mean voltages in the FG groups were at least 2.7 times higher than those in the CG. The power densities, current densities, and polarization curves of the five CW-MFC reactors are shown in Fig. 5b. The maximum power densities and current densities of the

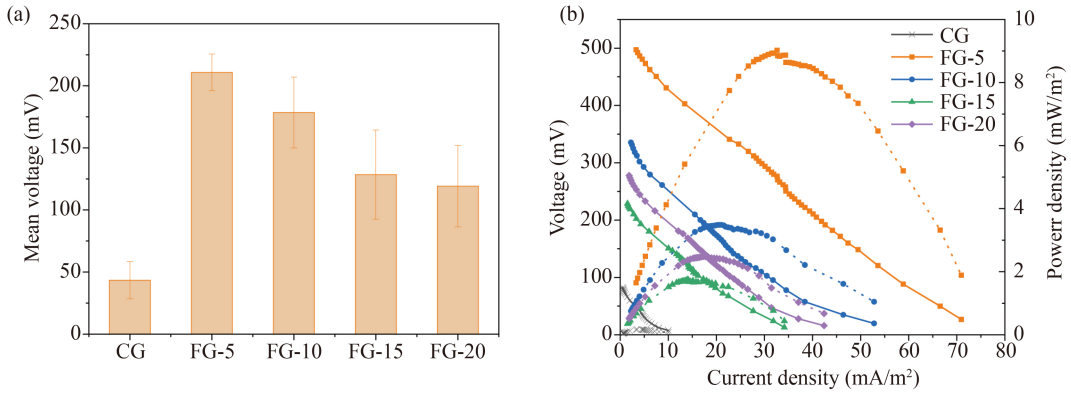

Fig. 5 Mean voltage (a), polarization curves and power density curves (b) of Period I. (CG: control group without fermentation broth, FG-5: fermentation group added with 5 d fermentation broth, FG-10: fermentation group added with 10 d fermentation broth, FG-15: fermentation group added with 15 d fermentation broth, FG-20: fermentation group added with 20 d fermentation broth).

five CW-MFCs are as follows: FG-5 > FG-10 > FG-20 > FG-15 > CG. FG-5 possessed the highest power density of 9.02 mW/m^2, whereas the power density in CG was 0.17 mW/m^2. The peak current densities of CG, FG-5, FG-10, FG-15, and FG-20 were 10.00, 70.93, 52.80, 34.13, and 42.40 mA/m^2, respectively. In addition, the CE of CG, FG-5, FG-10, FG-15, and FG-20 were 2.03%, 5.09%, 4.16%, 3.03%, and 2.88%, respectively. The internal resistance of the CG was 900 Ω, whereas the internal resistance of all FG groups was less than 600 Ω.

The bioelectricity performance of the CW-MFCs in Period II is summarized in Table 1. The mean voltages of CG', Ac, and Ac&HA were 24.53, 123.81, and 149.21 mV, respectively. Obviously, with the addition of Ac and HA, the mean voltages of the CW-MFCs increased. The internal resistance of Ac&HA, which was 275 Ω, was the lowest, and the internal resistances of CG' and Ac were 650 and 375 Ω, respectively. The power densities of CG', Ac, and Ac&HA were 0.02, 9.91, and 11.01 mW/m^2, respectively. The current densities of CG', Ac, and Ac&HA were 3.47, 88.27, and 92.53 mW/m^2, respectively. The CEs of CG', Ac, and Ac&HA were 1.09%, 3.13%, and 3.87%, respectively. The mean voltage, power density, current density, and CE of Ac, Ac&HA were significantly higher than those of CG'.

3.4 Bacterial diversity and community distribution

The relative community abundances at the phylum level are shown in Fig. 6a. The seven most abundant phyla were *Proteobacteria* (24.78%–30.37%), *Chloroflexi* (22.24%–25.17%), *Bacteroidota* (11.74%–13.89%), *Patescibacteria* (8.18%–9.78%), *Acidobacteriota* (4.69%–6.91%), *Planctomycetota* (3.54%–5.10%), and *Actinobacteriota* (2.53%–4.44%). *Proteobacteria*, the dominant phylum in the three reactors, had the highest abundance in the CG' (30.37%), followed by Ac&HA (28.49%) and Ac (24.78%). The abundance of microorganisms at the family level is shown in Fig. 6b. *Rhodocyclaceae, Anaerolineaceae,* SC-I-84*, Comamonadaceae, and Saprospiraceae* were the dominant families in the CG', Ac, and Ac&HA systems. *Rhodocyclaceae* had the highest abundance, accounting for 13.18%, 11.10%, and 9.70% in CG', Ac, and Ac&HA, respectively.

To further understand the nitrogen metabolism in CW-MFCs, we utilized PICRUSt2 to predict the functional gene abundances associated with denitrification and nitrification (Fig. 6c and Fig. S2). Obviously, the relative abundances in Ac&HA significantly exceeded those of Ac and CG'. The relative abundance of nitrate reductase in Ac&HA was approximately 0.04%, which was 1.5 times as much as that in Ac and CG'. Furthermore, the addition of Ac and HA did not promote nitrification and reduced the abundance of the nitrification genes (showed in Fig. S2). The relative abundances of extracellular electron transfer (EET) functional genes in CG', Ac, and Ac&HA were 1.16%, 1.24%, and 1.20%, respectively (Fig. 6d). EET functional genes were enriched in Ac and Ac&HA.

Table 1 Bioelectricity performance of CW-MFCs in Period II

Indicators	CG'	Ac	Ac&HA
Mean voltage (mV)	24.53 ± 0.01	123.81 ± 0.03	149.21 ± 0.01
Internal resistance (Ω)	650	375	275
Maximum power density (mW/m^2)	0.02	9.91	11.01
Maximum current density (mA/m^2)	3.47	88.27	92.53
Coulombic efficiency (%)	1.09	3.13	3.87

Note: CG' denotes control group without Ac and HA, Ac denotes added with 30 mg/L Ac, Ac&HA denotes added with 30 mg/L Ac and 2.5 mg/L HA.

4 Discussion

4.1 Enhancement of pollutant removal in CW-MFC with fermentation broth

4.1.1 COD removal

The COD removal effects of Periods I (Fig. 3a) and II (Fig. 4a) were analogous; the removal efficiency of CG

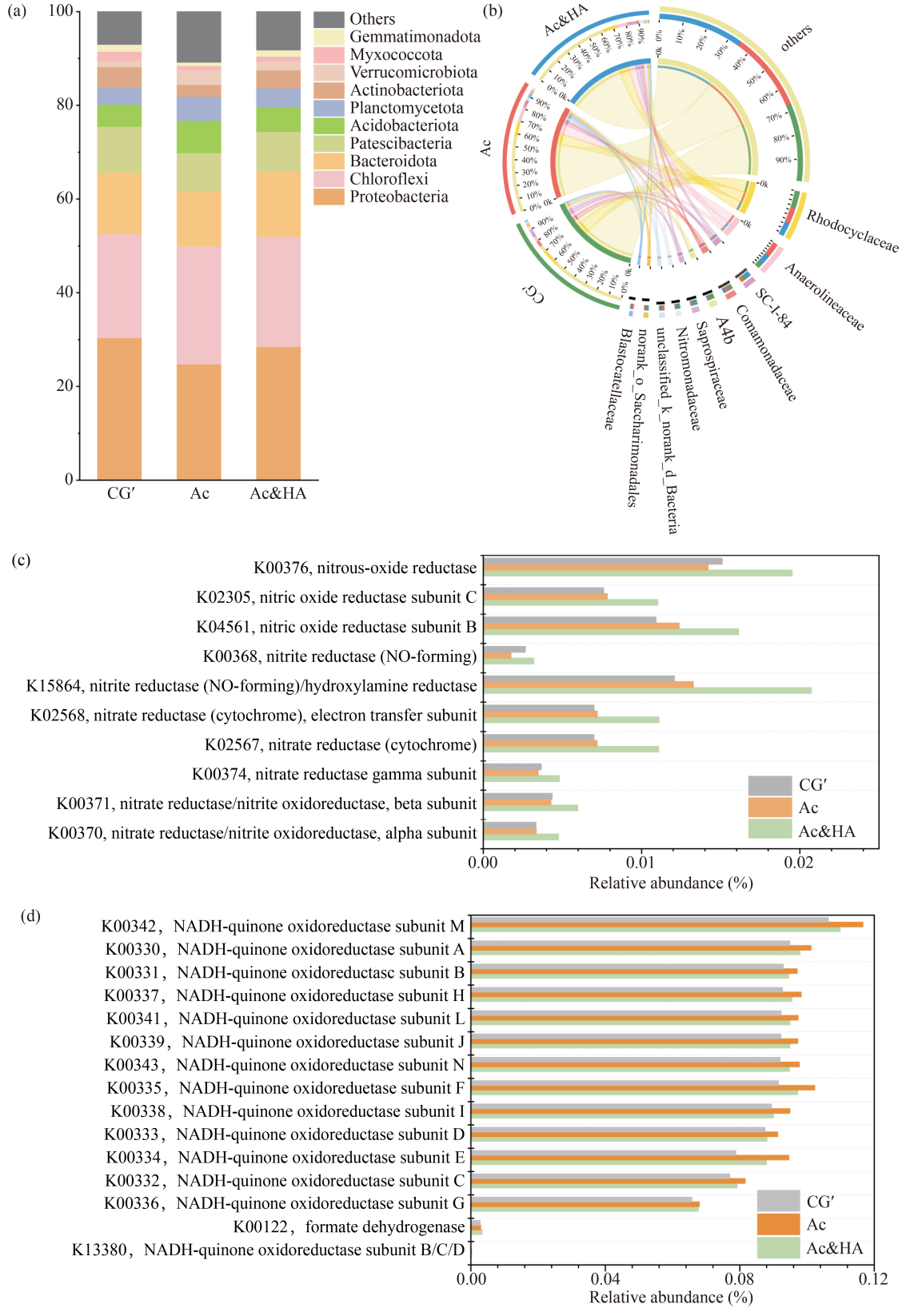

Fig. 6 Relative abundance of bacterial community at phylum (a) and family (b) in Period II; functional genes abundances related to denitrification (c) and electron transfer (d) were predicted with PICRUSt2. (CG': control group without Ac and HA, Ac: added with 30 mg/L Ac, Ac&HA: added with 30 mg/L Ac and 2.5 mg/L HA).

(or CG') was significantly inferior to that of the other groups. The fermentation broths were considered to facilitate COD removal from two aspects: they strengthened the EET process (showed in Fig. 5a and Table 1) and denitrification process (Fig. 3 and Fig. 4). Carbon source in the fermentation broths increases the activity of microorganisms (Deng et al., 2011) and exacerbates hypoxic conditions (Table 2), which promotes denitrification. Furthermore, Huang et al. (2019) proved that HA boosted the electron transfer efficiency between the electrode and microbes because it could reduce the metabolic overpotential of microorganisms, and abundant COD was consumed during this process. Consequently, the EET and denitrification processes promoted COD removal. The addition of fermentation broths in CW-MFCs that treat tail water does not cause secondary pollution, because of the high COD removal efficiency.

4.1.2 Nitrogen removal

Studies have indicated that adding carbon sources has little influence on NH_4^+-N removal (Zhu et al., 2014). This conclusion was demonstrated in Period I (Fig. 3b). The addition of carbon sources aggravated the anaerobic conditions inside the systems, and the nitrification process needed to be conducted under aerobic conditions (Fu et al., 2017). The abundance of functional genes associated with nitrification was predicted using the PICRUSt2 (Wu et al., 2022).

The removal efficiency of NO_3^--N increased significantly after the addition of carbon sources. The differences between CG (or CG') and the other groups were mainly reflected in COD/NO_3^--N. In this study, the NO_3^--N concentration of the influent remained stable, whereas the COD concentration of the influent increased. This result confirmed that a high COD/NO_3^--N could promote denitrification (Zhu et al., 2014). The relative abundances of *Proteobacteria, Bacteroidetes*, and *Chloroflexi* in Ac&HA were higher than those in Ac (Fig. 6a), and these phyla were assumed to be possible for denitrification (Hua et al., 2018). HA could be considered an additive that enhances the relative abundance of nitrogen removal microorganisms when combined with Ac.

Plant fermentation broths were propitious to further remove NO_3^--N and TN in CW-MFCs by taking advantage of plant fermentation broths to resolve the issue of unstable carbon supply (Chen et al., 2014a), which studies on solid carbon sources for denitrification have observed. For example, Si et al. (2018) utilized wheat straw and cotton as carbon sources to compare denitrification rates. Tao et al. (2021) used NaOH heat-pretreated corn stalks as a carbon source to further treat low C/N wastewater. However, this addition method leads to an excessive carbon supply in the initial stage. Only a few carbon sources were used for denitrification.

The TN removal performances of FG-15 and FG-20 were better than those of FG-5 and FG-10 in Period I because of the presence of HA. TN removal rates of Ac and Ac&HA were higher than CG', which increased the TN removal efficiencies by more than 12.5% (as showed in Fig. 4d). Moreover, Ac&HA had higher removal efficiencies than Ac, indicating that the combination of Ac and HA can achieve the most efficient denitrification. The main function of HA is to enhance the electron transfer efficiency because the metabolic overpotential of microorganisms is reduced by HA (Huang et al., 2019), and the electrons would drive the denitrification process. Therefore, electrochemistry can promote the denitrification process (Ma et al., 2015). There was a mutual promotion relationship between Ac and HA during denitrification, which is also confirmed by Fig. 6c. The abundance of functional genes associated with denitrification was predicted using PICRUSt2 (Liang et al., 2021). After adding HA, the abundances of nitrous-oxide reductase, nitric oxide reductase, nitrite reductase, nitrate reductase, and nitrate reductase/nitrite oxidoreductase were much higher than those of CG' and Ac. The nitrogen metabolism genome is well developed and highly

Table 2 Effluent parameters of different groups during the experiment

Groups		COD (mg/L)	NH_4^+-N (mg/L)	NO_3^--N (mg/L)	TN (mg/L)	pH	DO (mg/L)
Period I	CG	14.72 ± 0.66	4.35 ± 0.74	3.24 ± 0.03	7.59 ± 0.55	8.33	0.66
	FG-5	7.55 ± 1.56	4.32 ± 0.56	0.13 ± 0.07	5.02 ± 0.61	7.39	0.27
	FG-10	5.83 ± 0.39	4.13 ± 0.15	0.15 ± 0.03	4.43 ± 1.14	7.20	0.30
	FG-15	6.00 ± 0.49	2.85 ± 0.91	0.19 ± 0.01	3.47 ± 1.13	7.35	0.25
	FG-20	3.03 ± 0.24	3.48 ± 0.38	0.18 ± 0.04	3.90 ± 0.51	7.22	0.21
Period II	CG'	13.48 ± 0.16	3.61 ± 0.88	3.24 ± 0.72	7.03 ± 1.44	8.11	0.62
	Ac	3.55 ± 0.73	3.56 ± 0.52	0.35 ± 0.24	4.28 ± 0.58	7.62	0.23
	Ac&HA	8.74 ± 0.90	3.21 ± 0.66	0.22 ± 0.09	3.05 ± 0.41	7.32	0.21

Note: CG denotes control group without fermentation broth, FG-5 denotes fermentation group added with 5 d fermentation broth, FG-10 denotes fermentation group added with 10 d fermentation broth, FG-15 denotes fermentation group added with 15 d fermentation broth, FG-20 denotes fermentation group added with 20 d fermentation broth, CG' denotes control group without Ac and HA, Ac denotes added with 30 mg/L Ac, Ac&HA denotes added with 30 mg/L Ac and 2.5 mg/L HA.

accurate. However, the prediction of PICRUSt2 is biased toward the existing genome; thus, identifying rare functional genes is difficult. Besides, predictions cannot provide resolution to distinguish strain-specific function (Douglas et al., 2020). Therefore, it is necessary to determine whether the genome can be accurately classified before prediction.

4.2 Enhancement of power generation in CW-MFC with fermentation broth

The addition of fermentation broths could significantly improve the electricity production capacities of CW-MFC systems (Fig. 5a). The highest output voltage reached 210.85 mV after adding fermentation, and the influent COD concentration was around 90 mg/L in FGs. Wang et al. (2019) chose sodium acetate as carbon source, and the output voltage was less than 150 mV in the same COD concentration. It showed that fermentation broth is more beneficial for electricity generation.

FG-5 had the highest voltage for two reasons: the components of fermentation broths at the early stage were easy to utilize, and carbon sources preferentially acted on denitrification rather than electricity generation when HA existed. FG-5 had the highest voltage, which was improved 167.42 mV than CG. Although the promotion effect gradually decreased with an increase in the fermentation period, the voltage of FG-20 was still 75.75 mV higher than that of CG. With the extension of the fermentation period, the carbon sources gradually transformed from short-chain fatty acids to refractory humic substances (Zheng et al., 2021), which led to restrictions in the process of electroactive bacteria using carbon sources to generate electricity. However, the electrogenic performance of Ac&HA was better than that of Ac (Table 1), which indicated that HA could further enhance electricity production when the influent Ac concentrations remained stable. HA can promote electron transfer efficiency because the metabolic overpotential of microorganisms is reduced by HA (Huang et al., 2019).

Furthermore, the mean voltages of the fermentation groups in Period I exhibited a stepped-downward trend. However, both the VFA (shown in Fig. S1) and the removal efficiencies of TN (Fig. 3) increased. This finding might illustrate that the carbon sources preferentially act on the denitrification process rather than on the electricity generation process. Homologous conclusions could be drawn from the PICRUSt2 results that the addition of HA greatly improved the abundance of functional genes related to denitrification rather than the abundance of functional genes related to electron transfer.

4.3 Environmental significance

Nitrogen residues in the secondary effluents of WWTPs might cause eutrophication in receiving water bodies (Zhou et al., 2021). The addition of a carbon source is a commonly used method for removing nitrogen residues. However, soluble carbon sources are expensive and may cause secondary pollution (Yuan et al., 2020), and inappropriate supplementation of solid carbon would result in the clogging of reactors (Zhao et al., 2017). The use of fermentation broth as a liquid carbon source can effectively avoid these problems. In this study, wetland plant litter fermentation broth was used as an additional carbon source and added to the CW-MFC reactors to improve the advanced treatment of nitrogen in the secondary effluent and strengthen the electricity generation performance.

The results showed that the wetland plant litter fermentation broth was an effective external carbon source, which solved the problem of carbon source waste. The wetland is a carbon sink with a plant litter accumulation rate of 500–2000 g C/(m^2·yr) (Hume et al., 2002), and these abundant carbon sources could not be released into the CWs, because of the barrier of surface gravel layers. In this study, fermentation broths were made by wetland plant litter to motivate the recycling of waste carbon sources, which have the advantages of being readily accessible, simple operation, and low cost. The effluent quality improved after the treatment with CW-MFC reactors, which greatly reduced the environmental risk caused by nitrogen residues. For instance, the lowest concentration of NO_3^--N reached 0.13 mg/L (Table 2). In addition, the maximum mean voltage reached 210.85 mV, indicating that CW-MFCs have substantial potential for energy production. According to our research, ecological technologies such as CW-MFC should be vigorously promoted to dispose of secondary effluents from WWTPs.

5 Conclusions

The aquatic ecosystem is harmed by nitrogen residues in the secondary effluent of WWTPs, and the addition of a carbon source is the most commonly used for advanced nitrogen removal. In this study, 5–20 d fermentation broths were prepared and added to CW-MFC reactors. The consequences in Period I showed that FG-15 had the best effect on enhanced denitrification, which could increase the removal efficiency of TN by 19.60% than CG. The FG-5 improved bioenergy generation most, which was 167.42 mV higher than that of CG. The carbon source preferentially acted on denitrification rather than on electricity generation. A mutual promotion relationship between Ac and HA in nitrogen removal was observed using PICRUSt2. This experiment realized simultaneous denitrification and bioenergy generation of secondary effluent, which is beneficial for alleviating water eutrophication.

Acknowledgements This work was supported by the National Natural Science Foundation of China (No. U20A20326), the Fundamental Research

Funds for the Central Universities (No. 2020CDJDPT002), and Chongqing Talents Plan for Young Talents (No. CQY201905062).

Electronic Supplementary Material Supplementary material is available in the online version of this article at https://doi.org/10.1007/s11783-022-1592-x and is accessible for authorized users.

References

APHA (1998). Standard Methods for the Examinations of Water and Wastewater. Washington, DC: American Public Health Association

Chen M, Chang L, Zhang J, Guo F, Vymazal J, He Q, Chen Y (2020). Global nitrogen input on wetland ecosystem: The driving mechanism of soil labile carbon and nitrogen on greenhouse gas emissions. Environmental Science and Ecotechnology, 4: 100063

Chen Y, Wen Y, Zhou J, Tang Z, Li L, Zhou Q, Vymazal J (2014a). Effects of cattail biomass on sulfate removal and carbon sources competition in subsurface-flow constructed wetlands treating secondary effluent. Water Research, 59: 1–10

Chen Y, Wen Y, Zhou Q, Vymazal J (2014b). Effects of plant biomass on nitrogen transformation in subsurface-batch constructed wetlands: a stable isotope and mass balance assessment. Water Research, 63: 158–167

Dash B P, Chaudhari S (2005). Electrochemical denitrificaton of simulated ground water. Water Research, 39(17): 4065–4072

Deng H, Ge L, Xu T, Zhang M, Wang X, Zhang Y, Peng H (2011). Analysis of the metabolic utilization of carbon sources and potential functional diversity of the bacterial community in lab-scale horizontal subsurface-flow constructed wetlands. Journal of Environmental Quality, 40(6): 1730–1736

Douglas G M, Maffei V J, Zaneveld J R, Yurgel S N, Brown J R, Taylor C M, Huttenhower C, Langille M G I (2020). PICRUSt2 for prediction of metagenome functions. Nature Biotechnology, 38(6): 685–688

Duan Y, Zhou A, Wen K, Liu Z, Liu W, Wang A, Yue X (2019). Upgrading VFAs bioproduction from waste activated sludge via co-fermentation with soy sauce residue. Frontiers of Environmental Science & Engineering, 13(1): 3

Fu G, Huangshen L, Guo Z, Zhou Q, Wu Z (2017). Effect of plant-based carbon sources on denitrifying microorganisms in a vertical flow constructed wetland. Bioresource Technology, 224: 214–221

Fu G, Yu T, Huangshen L, Han J (2018). The influence of complex fermentation broth on denitrification of saline sewage in constructed wetlands by heterotrophic nitrifying/aerobic denitrifying bacterial communities. Bioresource Technology, 250: 290–298

Guo F, Xu F, Cai R, Li D, Xu Q, Yang X, Wu Z, Wang Y, He Q, Ao L, Vymazal J, Chen Y (2022). Enhancement of denitrification in biofilters by immobilized biochar under low-temperature stress. Bioresource Technology, 347: 126664

Hansen A T, Dolph C L, Foufoula-Georgiou E, Finlay J C (2018). Contribution of wetlands to nitrate removal at the watershed scale. Nature Geoscience, 11(2): 127–132

Hua G, Cheng Y, Kong J, Li M, Zhao Z (2018). High-throughput sequencing analysis of bacterial community spatiotemporal distribution in response to clogging in vertical flow constructed wetlands. Bioresource Technology, 248(Pt B): 104−112

Huang B, Fu G, He C, He H, Yu C, Pan X (2019). Ferroferric oxide loads humic acid doped anode accelerate electron transfer process in anodic chamber of bioelectrochemical system. Journal of Electroanalytical Chemistry (Lausanne, Switzerland), 851: 113464

Hume N P, Fleming M S, Horne A J (2002). Plant carbohydrate limitation on nitrate reduction in wetland microcosms. Water Research, 36(3): 577–584

Liang D, He W, Li C, Wang F, Crittenden J C, Feng Y (2021). Remediation of nitrate contamination by membrane hydrogenotrophic denitrifying biofilm integrated in microbial electrolysis cell. Water Research, 188: 116498

Luo Y, Zhang Y, Lang M, Guo X, Xia T, Wang T, Jia H, Zhu L (2021). Identification of sources, characteristics and photochemical transformations of dissolved organic matter with EEM-PARAFAC in the Wei River of China. Frontiers of Environmental Science & Engineering, 15(5): 96

Ma J, Wang Z, He D, Li Y, Wu Z (2015). Long-term investigation of a novel electrochemical membrane bioreactor for low-strength municipal wastewater treatment. Water Research, 78: 98–110

Oon Y L, Ong S A, Ho L N, Wong Y S, Dahalan F A, Oon Y S, Lehl H K, Thung W E, Nordin N (2018). Up-flow constructed wetland-microbial fuel cell for azo dye, saline, nitrate remediation and bioelectricity generation: From waste to energy approach. Bioresource Technology, 266: 97–108

Puig S, Coma M, Desloover J, Boon N, Colprim J, Balaguer M D (2012). Autotrophic denitrification in microbial fuel cells treating low ionic strength waters. Environmental Science & Technology, 46(4): 2309–2315

Si Z, Song X, Wang Y, Cao X, Zhao Y, Wang B, Chen Y, Arefe A (2018). Intensified heterotrophic denitrification in constructed wetlands using four solid carbon sources: Denitrification efficiency and bacterial community structure. Bioresource Technology, 267: 416–425

Tao Z, Jing Z, Wang Y, Tao M, Luo H (2021). Higher nitrogen removal achieved in constructed wetland with polyethylene fillers and NaOH-heating pre-treated corn stalks for advanced treatment of low C/N sewage. Environmental Science and Pollution Research International, 28(11): 13829–13841

Wang X, Feng Y, Wang H, Qu Y, Yu Y, Ren N, Li N, Wang E, Lee H, Logan B E (2009). Bioaugmentation for electricity generation from corn stover biomass using microbial fuel cells. Environmental Science & Technology, 43(15): 6088–6093

Wang X, Tian Y, Liu H, Zhao X, Wu Q (2019). Effects of influent COD/TN ratio on nitrogen removal in integrated constructed wetland-microbial fuel cell systems. Bioresource Technology, 271: 492–495

Wu Z, Gao J, Cui Y, Li D, Dai H, Guo Y, Li Z, Zhang H, Zhao M (2022). Metagenomics insights into the selective inhibition of NOB and comammox by phenacetin: Transcriptional activity, nitrogen metabolism and mechanistic understanding. Science of the Total Environment, 803: 150068

Yan J, Hu X, He Q, Qin H, Yi D, Lv D, Cheng C, Zhao Y, Chen Y (2021). Simultaneous enhancement of treatment performance and energy recovery using pyrite as anodic filling material in constructed wetland coupled with microbial fuel cells. Water

Research, 201: 117333

Yuan C, Zhao F, Zhao X, Zhao Y (2020). Woodchips as sustained-release carbon source to enhance the nitrogen transformation of low C/N wastewater in a baffle subsurface flow constructed wetland. Chemical Engineering Journal, 392: 124840

Zhang C, Yin Q, Wen Y, Guo W, Liu C, Zhou Q (2016). Enhanced nitrate removal in self-supplying carbon source constructed wetlands treating secondary effluent: The roles of plants and plant fermentation broth. Ecological Engineering, 91: 310–316

Zhao C, Shang D, Zou Y, Du Y, Wang Q, Xu F, Ren L, Kong Q (2020). Changes in electricity production and microbial community evolution in constructed wetland-microbial fuel cell exposed to wastewater containing Pb(II). Science of the Total Environment, 732: 139127

Zhao J, Mo F, Wu J, Hu B, Chen Y, Yang W (2017). Clogging Simulation of Horizontal Subsurface-Flow Constructed Wetland. Environmental Engineering Science, 34(5): 343–349

Zheng Y, Cao T, Zhang Y, Xiong J, Dzakpasu M, Yang D, Yang Q, Liu Y, Li Q, Liu S, Wang X (2021). Characterization of dissolved organic matter and carbon release from wetland plants for enhanced nitrogen removal in constructed wetlands for low C-N wastewater treatment. Chemosphere, 273: 129630

Zhou Z, Wang K, Qiang J, Pang H, Yuan Y, An Y, Zhou C, Ye J, Wu Z (2021). Mainstream nitrogen separation and side-stream removal to reduce discharge and footprint of wastewater treatment plants. Water Research, 188: 116527

Zhu H, Yan B, Xu Y, Guan J, Liu S (2014). Removal of nitrogen and COD in horizontal subsurface flow constructed wetlands under different influent C/N ratios. Ecological Engineering, 63: 58–63